Quaternary Research **56**, 366–382 (2001)
doi:10.1006/qres.2001.2278, available online at http://www.idealibrary.com on IDEAL®

Determination of ^{36}Cl Production Rates Derived from the Well-Dated Deglaciation Surfaces of Whidbey and Fidalgo Islands, Washington

Terry W. Swanson

Department of Geological Sciences and Quaternary Research Center, University of Washington, Box 35-1310, Seattle, Washington 98195

E-mail: tswanson@u.washington.edu

Marc L. Caffee

Center for Accelerator Mass Spectrometry, Lawrence Livermore National Laboratory, L-202, Livermore, California 94550

Received August 31, 1999

The ^{36}Cl dating method is increasingly being used to determine the surface-exposure history of Quaternary landforms. Production rates for the ^{36}Cl isotopic system, a critical component of the dating method, have now been refined using the well-constrained radiocarbon-based deglaciation history of Whidbey and Fidalgo Islands, Washington. The calculated total production rates due to calcium and potassium are 91 ± 5 atoms ^{36}Cl (g Ca)$^{-1}$ yr^{-1} and are 228 ± 18 atoms ^{36}Cl (g K)$^{-1}$ yr^{-1}, respectively. The calculated ground-level secondary neutron production rate in air, $P_f(0)$, inferred from thermal neutron absorption by ^{35}Cl is 762 ± 28 neutrons (g air)$^{-1}$ yr^{-1} for samples with low water content (1–2 wt.%). Neutron absorption by serpentinized harzburgite samples of the same exposure age, having higher water content (8–12 wt.%), is ~40% greater relative to that for dry samples. These data suggest that existing models do not adequately describe thermalization and capture of neutrons for hydrous rock samples. Calculated ^{36}Cl ages of samples collected from the surfaces of a well-dated dacite flow (10,600–12,800 cal yr B.P.) and three disparate deglaciated localities are consistent with close limiting calibrated ^{14}C ages, thereby supporting the validity of our ^{36}Cl production rates integrated over the last ~15,500 cal yr between latitudes of 46.5° and 51°N. Although our production rates are internally consistent and yield reasonable exposure ages for other localities, there nevertheless are significant differences between these production rates and those of other investigators.

Key Words: **^{36}Cl production rates; cosmogenic isotopes; deglaciation; Cordilleran Ice Sheet.**

INTRODUCTION

Chlorine-36 is one of several cosmogenic isotopes (i.e., ^{10}Be, ^{26}Al, ^{3}He, and ^{21}Ne) that are being used successfully to determine exposure histories for a diverse assemblage of Quaternary landforms (reviewed by Cerling and Craig, 1994). The accuracy of the results obtained using this method are dependent on a variety of geologic processes and physical parameters, production rates being a primary example of the latter. Errors in production rates can translate into significant errors in derived ages.

The nuclear processes that produce cosmogenic ^{36}Cl in rocks are spallation, neutron capture, and muon capture. The first two processes dominate production on the land surface; muon production in Ca and K becomes more important with increasing depth (Rama and Honda, 1961). The decay of radioactive U and Th also gives rise to the production of ^{36}Cl, via neutron capture (Bentley *et al.*, 1986). This subsurface ^{36}Cl, generally in secular equilibrium, can be subtracted from the total accelerator mass spectrometry (AMS)–measured ^{36}Cl to determine the cosmogenic component (Phillips *et al.*, 1986). The production rate of cosmogenic ^{36}Cl in bedrock and regolith exposed at Earth's surface is dependent on its calcium, potassium, and chloride content and can be expressed by the equation

$$P = \psi_{Ca}(\mathrm{C_{ca}}) + \psi_K(\mathrm{C_K}) + \psi_n(\sigma_{35}\,\mathrm{N_{35}}/\,\Sigma\sigma_i\mathrm{N_i}),$$

where ψ_K and ψ_{Ca} are the total production rates (including production due to slow negative muons) of ^{36}Cl due to potassium and calcium, respectively; C_K and C_{ca} are the elemental concentrations of potassium and calcium, respectively; and ψ_n is the thermal neutron capture rate, which is dependent on the fraction of neutrons stopped by ^{35}Cl ($\sigma_{35}\,N_{35}/\,\Sigma\sigma_i N_i$), as determined by the effective cross sections of ^{35}Cl (σ_{35}) and all other absorbing elements ($\Sigma\sigma$) and their respective abundances (N_{35} and N_i). The work reported here was originally motivated by the initial findings of Swanson *et al.* (1992). ^{36}Cl exposure ages of samples collected from deglaciated surfaces (i.e., ground moraine boulders and glacially abraded bedrock) in the northern Puget Sound region of Washington were 20–40% older than calibrated ^{14}C ages bracketing the time of deglaciation for this region. Swanson *et al.* (1992) concluded that the scaled production rates of Zreda *et al.* (1991) may have underestimated production for the samples collected in the Puget Lowland.

Zreda *et al.* (1991) were the first to calculate time-integrated production rates for cosmogenic ^{36}Cl using independently dated

Supplementary data from this article (Tables A1 and A2 in the Appendix) are available on IDEAL (http://www.idealibrary.com).

0033-5894/01 $35.00

TABLE 1
^{36}Cl Production Rate Calibration Studies

Study	Location	Altitude (m)	Latitude	Exposure age (10^3 yr)	Production rate[a] (atoms ^{36}Cl g^{-1} yr^{-1})
		Total production rate due to Ca [atoms ^{36}Cl (g Ca)$^{-1}$ yr^{-1}]			
This study	Puget Lowland, WA	10–140	47.5–48.4°N	15.5	91 ± 5
Phillips *et al.* (1996)	Varies	20–2578	20–80°N	3–55	72.5 ± 5
Stone *et al.* (1996)	Tabernacle Hill, UT	1445	38.9°N	17.3	53.6 ± 1.8
Zreda (1994)	Varies	20–2578	20–80°N	3–55	72.5 ± 5
		Total production rate due to K [atoms ^{36}Cl (g K)$^{-1}$ yr^{-1}]			
This study	Puget Lowland, WA	10–140	47.5–48.4°N	15.5	228 ± 18
Phillips *et al.* (1996)	Varies	20–2578	20–80°N	3–55	154 ± 10
Evans *et al.* (1997)	Sierra Nevada, CA; Scotland	3000–3600; 520	38°N; 58°N	13.1; 11.6	170 ± 27
Evans *et al.* (1997)	Antarctica	2000–2200	70°S	steady state	241 ± 9
Zreda (1994)	Varies	20–2578	20–80°	3–55	193 ± 20
		Secondary neutron production rate [neutron (g air)$^{-1}$ yr^{-1}]			
This study	Puget Lowland, WA	10–140	47.5–48.4°N	15.5	762 ± 28
Phillips *et al.* (1996)	Varies	20–2578	20–80°N	3–55	586 ± 40

[a] Production rate scaled to sea level and high geographic latitude (>60°).

geomorphic surfaces (Table 1). Since then, several other studies have undertaken the formidable task of determining production rates. The interpretation of many cosmogenic ^{36}Cl measurements is directly dependent on the accuracy of production rates. Accordingly, in the last decade many studies have been completed to assess production rates over diverse geographic and geologic settings (Table 1).

The lack of consistency between the various production rates reflects the numerous physical and geological processes affecting the production of ^{36}Cl. To some extent, a direct comparison of production rates is difficult, as these studies were conducted at different locations. A direct comparison is only possible after compensating or scaling for altitude and latitude. In some studies, the samples used to calculate a single production rate value were not collected from the same geographic setting (i.e., latitude and altitude) and were also integrated over different exposure histories. Finally, there is uncertainty regarding the validity of the independent chronology used to establish the baseline exposure age of the calibration surface in some of the production studies.

The well-dated retreat history of the Cordilleran Ice Sheet from the northern Puget Sound region of northwestern Washington (~15,500 cal yr B.P.) provides an exceptional opportunity to develop a set of production rates for the major ^{36}Cl production pathways. Because all of the calibration samples were collected from a closely limited geographic setting (47°–48°N and near sea level), the effects of latitude and altitude variation require little scaling, thereby eliminating one source of uncertainty. Furthermore, because all the samples were exposed about 15,500 cal yr B.P. at sites relatively close to 50°N latitude, the effect of secular variation in geomagnetic field strength is minor for the calibration samples.

The experimental work reported here includes both the actual determination of production rates and their subsequent validation. The production rates were determined using 50 calibration samples collected from northern Puget Lowland. The validation set consists of 23 samples collected from a late Pleistocene dacite flow in southwestern British Columbia and three disparate deglaciated localities in northern Washington and southern British Columbia. The dacite flow and the three deglaciation localities are dated by limiting ^{14}C ages.

METHODOLOGY

Rock samples were collected from moraine boulders and glacially abraded bedrock on Whidbey and Fidalgo Islands, Washington (Fig. 1). The sampling strategy maximized both sample size and lithologic diversity. The islands were selected as calibration locations for this study for following reasons.

1. Numerous ^{14}C ages have been obtained for organic matter beneath, within, and above the Vashon Till member of the Fraser Drift. Deglaciation of the islands occurred shortly before 13,470 ± 90 and 13,090 ± 90 ^{14}C yr B.P., based on ^{14}C ages of glacialmarine drift directly overlying Vashon till and organic sediments deposited in postglacial lakes (Fig. 2 and Table 2). These ages correspond to 16,275 (16,122) 15966 and 15,750 (15,578) 15,391 cal yr B.P., respectively (Stuiver *et al.*, 1998).

The calibrated ^{14}C age uncertainty for glacialmarine shells includes only the AMS and calibration uncertainty and likely underestimates the actual age uncertainty, the greatest source of which is probably related to the reservoir effect for shell ages in this region. Radiocarbon ages of gyttja and glacialmarine shells collected from a site in the north-central Puget Lowland

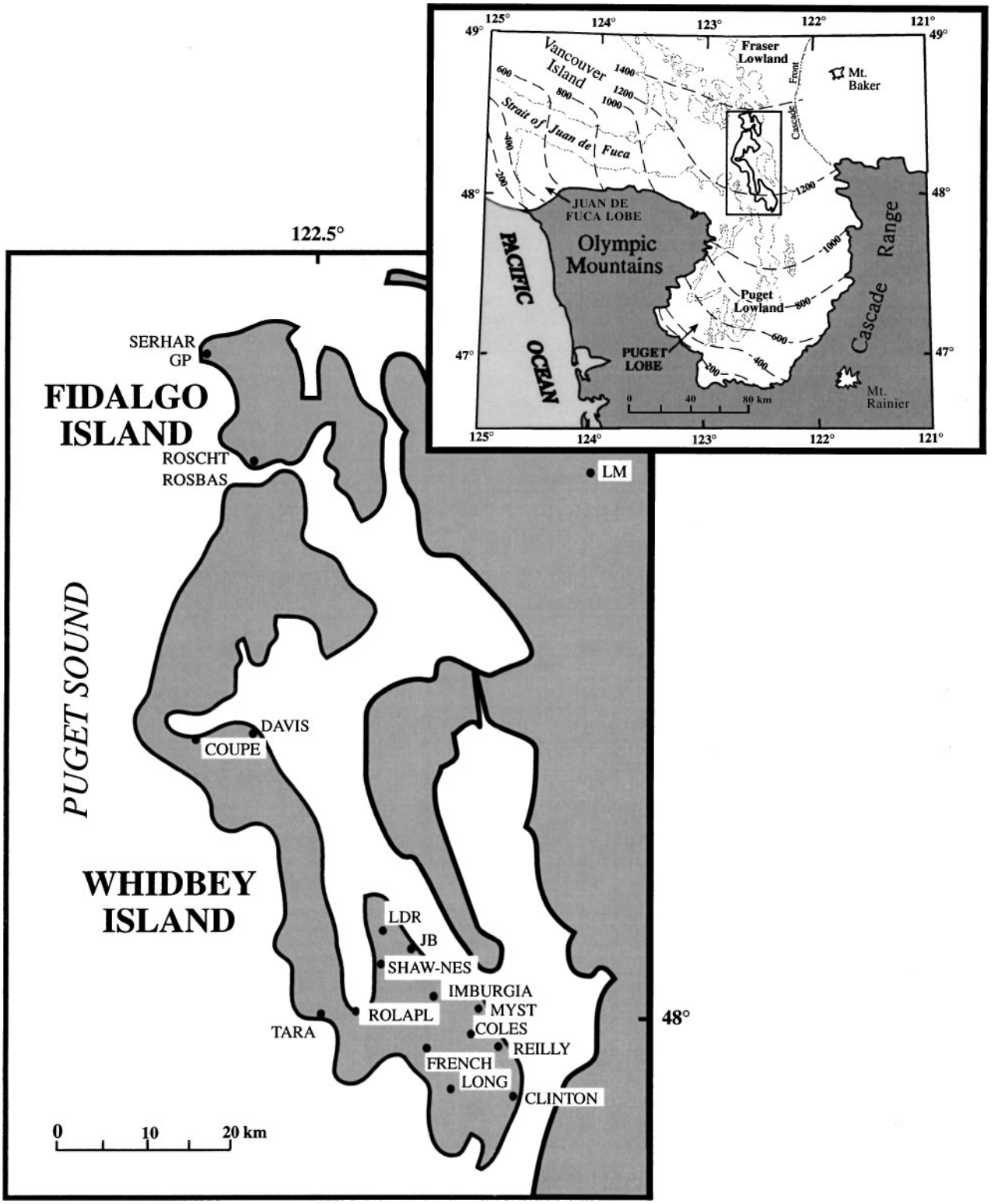

FIG. 1. Map of Whidbey and Fidalgo Islands showing localities where samples were obtained for the calibration of ^{36}Cl production parameters. Abbreviations correspond to sample names listed in Table 3 and Appendix (Supplementary Data). Inset index map of northwestern Washington and southwestern British Columbia shows the maximum extent of the Cordilleran Ice Sheet during the Vashon Stade of the Fraser Glaciation. Glacier contours (m), shown as dashed lines, is adapted from Thorson (1980).

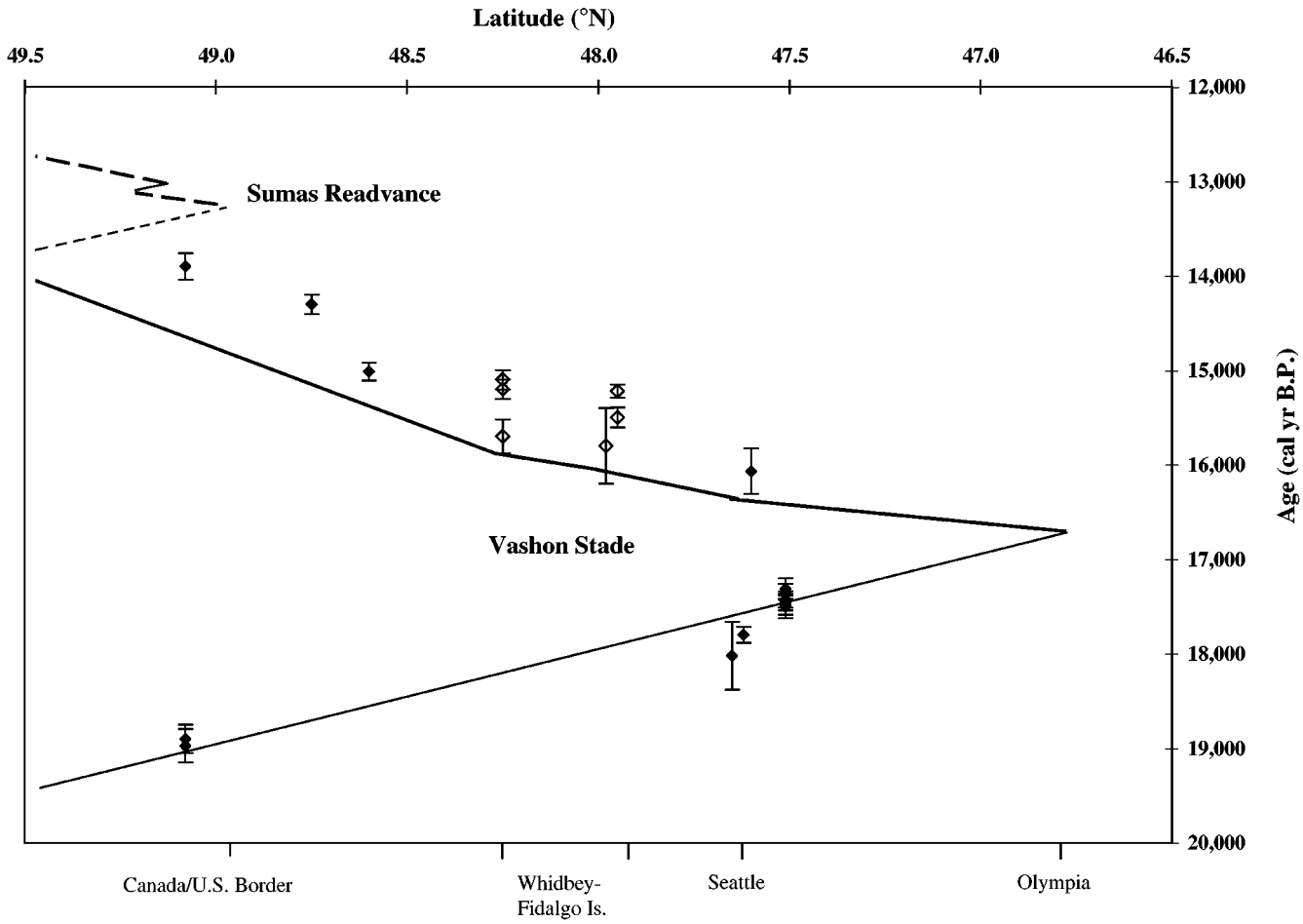

FIG. 2. Time–distance diagram showing the chronology of advance and retreat of the Cordilleran Ice Sheet into the Puget and Fraser Lowlands as constrained by close limiting ^{14}C ages. The ^{14}C ages used to construct this chronology are taken from Table 2. A 400-yr ^{14}C reservoir effect was assumed for glacialmarine drift shell ages (shown as open diamonds).

indicate that the reservoir effect may be <250 yr (Anundsen *et al.*, 1994). However, ^{14}C ages of wood and glacialmarine shells from a postglacial section near Deming, Washington, imply that the reservoir effect may be closer to 1000 yr (Table 2). The discrepancy between these two sites may reflect local differences in the mixing of upwelling marine water and glacial meltwater. Furthermore, the Deming region was deglaciated 800–1000 yr later than the central Puget Sound region, and ^{14}C production may have been lower at the time that the overlying glacialmarine shell unit was being deposited (J. Southon, personal communication, 1997). Here, we assume a reservoir effect of 400 yr for the calibration region.

2. The lithologic diversity of the deposits and bedrock provides a correspondingly diverse target composition for the production of ^{36}Cl. The accumulation area of the Puget Lobe lay in southwestern British Columbia and northwestern Washington (Booth, 1991). The bedrock geology of this region consists of allochthonous terranes that were accreted to western North America throughout the Cenozoic, as well as related autochthonous overlap sequences and plutons that define individual terrane boundaries (Brandon, 1989). The diversity in target composition permits the independent solution of a particular production parameter (i.e., spallation reactions for K and Ca or thermal activation of ^{35}Cl), and minimizes the uncertainty due to ^{36}Cl produced via the other production pathways.

3. The study region has been relatively stable since deglaciation. Tectonic offset of Late Pleistocene strata has been detected in only a few sites around the Puget Lowland (e.g., Bucknam *et al.*, 1992; Thorson, 1993). Postglacial uplift along local faults is inferred to be <10 m. Such displacement requires no altitude correction in calculating ^{36}Cl production rates. Although postglacial isostatic uplift was considerably greater than vertical tectonic offset, it likely occurred mainly as restrained rebound (Thorson, 1989; Dethier *et al.*, 1995) and has had a minimal effect on ^{36}Cl production.

4. Bracketing ^{14}C ages indicate that the retreat of the Puget Lobe was rapid across the study area (Porter and Swanson,

TABLE 2
Selected Radiocarbon Dates Constraining the Last Advance–Retreat Cycle of the Cordilleran Ice Sheet into the Puget Lowland, Washington, and Fraser Lowland, British Columbia

Laboratory number	Age ± 1σ (^{14}C yr B.P.)	Age (cal yr B.P.)[a]	Sample material	Latitude [°N]	Longitude [°W]	Location name	Source
			Sub-Vashon till samples (British Columbia)				
GSC-4335	16,000 ± 180	19,086 (18,876) 18,685	Spruce wood	49°05.1′	121°48.2′	Allison Pool	Clague *et al.* (1988)
GSC-4363	16,100 ± 150	19,168 (18,975)18,802	Spruce wood	49°05.1′	121°48.2′	Allison Pool	Clauge *et al.* (1988)
			Sub-Vashon till samples (Washington)				
W-1305	15,100 ± 300	18,330 (18,020)17,692	Detrital wood	47°37.5′	122°19.5′	Seattle	Mullineaux *et al.* (1965)
Beta-112019	14,890 ± 70	17,915 (17,799)17,687	Detrital wood	47°37.0′	122°11.5′	Bellevue	K. Troost, pers. comm. (1998)
QL-4620	14,570 ± 60	17,544 (17,437)17,331	Detrital wood	47°32.6′	122°01.5′	Issaquah delta	Porter and Swanson (1998)
CAMS-23177	14,550 ± 70	17,541 (17,426)17,312	Detrital wood	47°32.6′	122°01.5′	Issaquah delta	Porter and Swanson (1998)
CAMS-23176	14,480 ± 70	17,463 (17,347)17,331	Detrital wood	47°32.6′	122°01.5′	Issaquah delta	Porter and Swanson (1998)
CAMS-23175	14,600 ± 90	17,611 (17,481)17,352	Detrital wood	47°32.6′	122°01.5′	Issaquah delta	Porter and Swanson (1998)
CAMS-23171	14,580 ± 70	17,573 (17,459)17,346	Detrital wood	47°32.6′	122°01.5′	Issaquah delta	Porter and Swanson (1998)
CAMS-23170	14,620 ± 100	17,643 (17,503)17,365	Detrital wood	47°32.6′	122°01.5′	Issaquah delta	Porter and Swanson (1998)
CAMS-23160	14, 450 ± 90	17,446 (17,313)17,182	Detrital wood	47°32.6′	122°01.5′	Issaquah delta	porter and Swanson (1998)
			Post-Vashon till samples (Washington)				
QL-4069	13,700 ± 100	16,577 (16,422) 16,264	Freshwater gyttja	47°48.3′	122°31.3′	Lake Carpenter	Anundsen *et al.* (1994)
QL-1517	13,430 ± 200	16,349 (16,068) 15,771	Organic clay	47°38′	122°17′	Lake Washington	Leopold *et al.* (1982)
Beta-1319	13,650 ± 350	16,802 (16,358) 15,878	Glacialmarine shells	47°58′	122°32′	Oak Harbor	Dethier *et al.* (1995)
Beta-1716	13,600 ± 150	16,507 (16,294) 16,074	Glacialmarine shells	48°14′	122°42′	Oak Harbor	Dethier *et al.* (1995)
AA-10077	13,470 ± 90	16,275 (16,122) 15,966	Glacialmarine shells	47°58′	122°43′	Basalt Point	This study
QL-4608	12,260 ± 60	15,962 (15,830) 15,697	Glacialmarine shells	47°58′	122°32′	Double Bluff	This study
PC-01 (UWAMS)	13,230 ± 90	15,951 (15,787) 15,618	Glacialmarine shells	48°14′	122°42′	Penn Cove	This study
PC-02 (UWAMS)	13,090 ± 90	15,750 (15,578) 15,391	Glacialmarine shells	48°14′	122°42′	Penn Cove	This study
AA-22198	12,380 ± 90	15,370 (15,012) 14,655	Branch in basal peat	48°45′	122°07′	Nooksak River, WA	Kovanen and Easterbrook (2001)
AA-27076	12, 596 ± 90	14,480 (14,304) 14,115	Branch in basal peat	48°45′	122°07′	Nooksak River, WA	Kovanen and Easterbrook (2001)
GSC-3306	11, 900 ± 120	13,700 (13,380) 14,060	Branch in lake muds	49°04.5′	121°41.4′	Fraser Lowland, B.C.	Clague *et al.* (1997)

[a] Calibrated ^{14}C age calculations based on Stuiver *et al.* (1998).

1998). The average retreat rate likely exceeded 300 m yr^{-1} (Porter and Swanson, 1998). Accordingly, we infer that the ^{36}Cl ages for the entire study region represent broadly synchronous exposure ages encompassing less than ~300 yr of transgressive northerly retreat.

Sample Collection

Samples were chipped from the center of the top surface of boulders using a sledge hammer and mason's chisel. Where possible, less than 1 cm of the boulder's uppermost surface was collected to minimize scaling for depth-dependent complexities of ^{36}Cl production (Liu *et al.*, 1994). Samples were collected only from relatively flat surfaces (<15°) to minimize corrections for effects of surface geometry; these corrections for partial shielding are less than 0.4% for all samples. Because the ice sheet overrode much of its bedrock source region, most erratics excavated from the accumulation area were transported subglacially and are inferred to have been shielded from cosmic ray exposure until deglaciation.

Sampled boulders had diameters >1.5 m; boulders this large likely have not moved since deposition (Fig. 3). Many fine-grained lithologies (i.e., metavolcanic, chert, quartzite, argillite) have retained glacial striations, indicating little postdepositional surface erosion. Grooves preserved on some bedrock surfaces (e.g., arkosic sandstone, granite, and quartzite) show that the rate of surface erosion due to chemical and mechanical weathering processes has been low for most of the calibration samples (Fig. 4). Spalling on the sides of some erratic boulders likely is related to forest fires and was qualitatively evaluated in this study.

Chemical Analyses

Major elemental composition of rock samples was determined by X-ray fluorescence (XRF) spectrometry, with an analytical uncertainty of <2% and a detection limit of 0.01%. Analyses for boron and gadolinium (having large cross-section areas for neutrons) concentrations were measured by prompt gamma emission spectrometry, with an analytical uncertainty of <2% and a

FIG. 3. Most of the erratics used for calibration purposes in this study have diameters of >1.5 m and lie on relatively flat surfaces. This greenstone erratic (sample site JB-1; Fig. 1) is ~10 m high and was transported subglacially >50 km from its source on Mt. Erie, Fidalgo Island. Glacial grooves and striations are preserved on the upper surface of this erratic, as shown in this photograph. A person is shown for scale at the bottom of the photograph.

detection limit of 0.5 ppm. Uranium and thorium contents were determined by neutron activation, with an analytical uncertainty of <2% and a detection limit of 0.5 ppm. Chemical analyses were performed by XRAL laboratories (Don Mills, Ontario, Canada). Total chlorine content was determined by combination ion-selective electrode using modified procedures discussed by Aruscavage and Campbell (1983). Five or more replicates of each sample were measured to attain an analytical uncertainty of <5%. For low chloride concentrations (<15 ppm), up to 25 replicates of each sample were run to attain an uncertainty of <5%.

Sample Preparation and AMS Isotopic Analysis of ^{36}Cl

To extract Cl from silicate rock in a form suitable for accelerator mass spectrometry measurement, a wet chemical technique was used (Swanson, 1994), modified from a procedure outlined by Zreda *et al.* (1991).

The samples were analyzed for ^{36}Cl by accelerator mass spectrometry on a tandem Van de Graaf accelerator in the Center for Accelerator Mass Spectrometry (CAMS) at the Lawrence Livermore National Laboratory, Livermore, California (Davis *et al.*, 1990). Analytical uncertainties (1σ) of the AMS measurements were typically 2–5%.

Consistency of Results

The validity of the results was assessed using two independent data sets. Samples collected in the northern Puget Lowland had

FIG. 4. Glacial grooves and striations are preserved on the bedrock surfaces of many of the more resistant lithologies, such as this quartzite near Deception Pass, Washington. Chisel (chisel is parallel to ice flow direction) and hammer provide scale.

appropriate target element concentrations to serve as production rate calibration samples. Additional samples were collected and measured from the calibration area to assess the internal consistency of the production rates. To assess the applicability of the derived production rates to different geographic locations and exposure histories, we sampled a ^{14}C-dated dacite flow (10,600–12,800 cal yr B.P.) near Squamish, British Columbia, and three deglacial localities: the southernmost and oldest were near the terminal limits of the Puget and Okanogan lobes in Washington, and the youngest and northernmost were in the Interior Plateau region of British Columbia. These surfaces are independently dated by limiting ^{14}C ages.

^{36}Cl Production Rate Calculations

Calibration samples were divided into three groups based on target element concentrations so that the three principal ^{36}Cl production pathways (Ψ_{Ca}, Ψ_K, and Ψ_n) could be solved individually. Chemical and isotopic data for the calibration samples are shown in Table A1 of Appendix (Supplementary Data). Sample locations, shielding and scaling factors, and geologic data are shown in Table 3 and Figure 1. Background production of ^{36}Cl (R_o) from thermal neutrons produced by natural U and Th decay was calculated using the procedure described by Fabryka-Martin (1988). Production resulting from thermal neutron absorption by ^{35}Cl was treated using equations in Liu *et al.* (1994), which also were incorporated in recent calibrations of the ^{36}Cl production rates (e.g., Phillips *et al.*, 1996; Stone *et al.*, 1996). The production rate solution for a given reaction pathway was calculated using the CHLOE (Chlorine-36 exposure) program (Phillips and Plummer, 1996) and taking the collective mean value of all samples within each respective target element group. Individual production rate values were entered into CHLOE and solved minimizing the difference between calculated ages and the independent age of the calibration location (~15,500 cal yr). CHLOE treats production of ^{36}Cl using the neutron production and diffusion model developed by Liu *et al.* (1994). In this model Ψ_n depends on the chemical composition of each sample, so for the purpose of calibration we solved for the ground-level secondary neutron production rate in air, $P_f(0)$. This parameter is independent of sample composition but varies with altitude and latitude like an isotope production rate. Once calibrated, it can be used to determine Ψ_n for any sample composition (Liu *et al.*, 1994). Erosion rates entered in CHLOE ranged between 0.10 and 0.25 cm $(10^3 \text{ yr})^{-1}$. These values were based on field observations for the surface characteristics of boulders and abraded bedrock (i.e., presence or absence of striations and relief of quartz veins).

RESULTS AND DISCUSSION

The first target element group consisted of samples that possess low Ca/Cl and K/Cl ratios (Table A1 of Appendix); neutron activation of ^{35}Cl (Ψ_n) is the dominant ^{36}Cl production pathway for these samples. Total chlorine concentration of the samples ranges between 42 and 290 ppm. Water content varies considerably between the serpentinized harzburgite (10–12%) and the chert and diorite samples (~1–2%). As shown by Dep *et al.* (1994), water content may have a significant impact on the relative thermal neutron flux and, correspondingly, on ^{36}Cl production from this pathway. The Ψ_n reaction for these high chloride rock samples represents 65–98% of their respective total ^{36}Cl production (Table 3).

TABLE 3
Lithology, Altitude, Location, Thickness Averaged Production Rates, ^{36}Cl Ratios and Ages of Calibration Samples from Whidbey and Fidalgo Islands, Washington

Sample ID[a]	Sample type	Lithology	Altitude [m]	Latitude [°N]	Longitude [°W]	^{36}Cl/Cl (10^{-15})	^{36}Cl age $\pm 1\sigma$ (10^3 yr)	Thickness averaged production rates [atoms ^{36}Cl $(g * yr)^{-1}$]		
								ΨCa	ΨK	ΨN
SERHAR-1	Bedrock	Harzburgite	61	48°29.5′	122°41.5′	64.7 ± 5.5	15.7 ± 1.3	0.108	0.178	14.562
SERHAR-1b	Bedrock	Harzburgite	61	48°29.5′	122°41.5′	69.8 ± 2.6	16.7 ± 0.6	0.108	0.178	14.562
SERHAR-2	Bedrock	Harzburgite	61	48°29.5′	122°41.5′	62.9 ± 5.7	15.2 ± 1.4	0.095	0.198	13.730
SEHRAR-2A	Bedrock	Harzburgite	61	48°29.5′	122°41.5′	63.3 ± 14.0	15.2 ± 3.3	0.095	0.198	13.730
SERHAR-2B	Bedrock	Harzburgite	61	48°29.5′	122°41.5′	62.6 ± 3.7	15.2 ± 0.9	0.095	0.198	13.730
SERHAR-3	Bedrock	Harzburgite	61	48°29.5′	122°41.5′	63.8 ± 5.8	16.2 ± 1.5	0.014	0.218	13.923
SERHAR-3A	Bedrock	Harzburgite	61	48°29.5′	122°41.5′	66.1 ± 5.9	16.6 ± 1.5	0.014	0.218	13.923
SERHAR-3B	Bedrock	Harzburgite	61	48°29.5′	122°41.5′	65.0 ± 3.5	16.4 ± 0.9	0.014	0.218	13.923
CLINTON-3	Erratic	Greeanstone	42	47°56.5′	122°24.6′	64.9 ± 4.4	14.9 ± 1.0	8.571	0.193	12.926
LDR-1A	Erratic	Granodiorite	91	48°03.7′	122°29.9′	69.0 ± 8.6	15.3 ± 1.94	4.242	2.072	12.11
LDR-1B	Erratic	Granodiorite	91	48°03.7′	122°29.9′	72.2 ± 5.6	16.2 ± 1.3	4.249	2.127	11.426
LDR-1C	Erratic	Granodiorite	91	48°03.7′	122°29.9′	71.1 ± 4.8	15.8 ± 1.1	4.242	2.186	11.477
MYST-2	Erratic	Greenstone	56	48°02.0′	122°25.2′	97.7 ± 4.9	15.2 ± 0.8	6.974	0.229	3.521
MYST-2B	Erratic	Greenstone	56	48°02.0′	122°25.2′	84.9 ± 4.2	15.5 ± 0.9	6.684	0.172	4.596
ROSCHT-2	Bedrock	Chen	25	48°25.0′	122°40.0′	73.2 ± 10.0	14.9 ± 2.0	0.019	1.090	1.978
ROSCHT-2B	Bedrock	Chert	25	48°25.0′	122°40.0′	77.1 ± 4.8	15.8 ± 0.9	0.019	1.090	1.984

TABLE 3—*Continued*

Sample ID[b]	Sample type	Lithology	Altitude [m]	Latitude [°N]	Longitude [°W]	^{36}Cl/Cl (10^{-15})	^{36}Cl age $\pm 1\sigma$ (10^3 yr)	Thickness averaged production rates [atoms ^{36}Cl (g ∗ yr)$^{-1}$] ΨCa	ΨK	ΨN
ROSBAS-2	Bedrock	Basalt	25	48°25.0′	122°40.0′	212 ± 29	15.0 ± 2.1	5.752	0.111	0.802
ROSBAS-3	Bedrock	Basalt	25	48°25.0′	122°40.0′	226 ± 14	16.2 ± 1.0	4.491	0.129	0.655
ROSBAS-4	Bedrock	Basalt	25	48°25.0′	122°40.0′	203 ± 23	16.3 ± 1.8	3.876	0.333	0.693
JB-1A	Erratic	Greenstone	55	48°03.7′	122°25.2′	139.1 ± 6.6	15.5 ± 0.7	11.007	0.057	3.834
JB-1A2	Erratic	Greenstone	55	48°03.7′	122°25.2′	134 ± 12	15.0 ± 1.3	11.007	0.057	3.834
JB-1B	Erratic	Greenstone	55	48°03.7′	122°25.2′	140 ± 6.4	14.7 ± 0.7	10.871	0.038	3.600
JB-2	Erratic	Greenstone	55	48°03.7′	122°25.2′	121 ± 11	14.6 ± 1.3	10.939	0.306	3.151
DAVIS	Erratic	Basalt	61	48°13.0′	122°37.5′	230 ± 16.0	15.4 ± 1.1	4.423	0.423	0.765
COUPE-2	Erratic	Greenstone	34	48°12.7′	122°41.2	260 ± 54	16.0 ± 3.3	4.802	0.757	1.083
MYST-1	Erratic	Greenstone	56	48°02.0′	122°25.2′	265 ± 21	15.9 ± 1.2	7.144	0.306	1.127
MYST-1B	Erratic	Greenstone	56	48°02.0′	122°25.2′	254 ± 13.0	16.2 ± 0.9	6.455	0.268	1.108
FRENCH-B	Erratic	Gabbro	101	47°57.4′	122°24.0′	544 ± 45	16.9 ± 1.4	9.753	0.099	0.794
Sample ID[c]	Sample type	Lithology	Altitude [m]	Latitude [°N]	Longitude [°W]	^{36}Cl/Cl (10^{-15})	^{36}Cl age $\pm 1\sigma$ (10^3 yr)	Thickness averaged production rates [atoms ^{36}Cl (g ∗ yr)$^{-1}$] ΨCa	ΨK	ΨN
Reilly-B94	Erratic	Granite	76	48°01.0′	122°24.5′	97 ± 17	16.9 ± 3.0	0.238	1.966	2.343
COLES-8	Erratic	Granodiorite	61	48°01.2′	122°25.5′	330 ± 30	15.9 ± 1.4	2.198	1.817	0.768
ROL-APL	Erratic	Aplite dike	10	48°01.0′	122°32.5′	577 ± 47	16.4 ± 1.3	0.662	8.382	0.650
ROSCHT 3B		Chert	25	48°25.0′	122°40.0′	193 ± 12	16.7 ± 1.0	0.096	1.504	0.503
GP-1	Erratic	Graywacke	61	48°29.5′	122°37.5′	97.0 ± 3.5	14.9 ± 0.5	3.094	4.453	2.975
GP-2	Erratic	Graywacke	61	48°29.5′	122°37.5′	283 ± 7.6	16.4 ± 0.4	0.135	4.167	0.689
LM-2	Bedrock	Arkosic ss	285	48°23.7′	122°18.5′	349 ± 15	15.1 ± 0.7	0.361	4.702	0.801
LM-3	Bedrock	Arkosic ss	285	48°23.7′	122°18.5′	448 ± 11	15.4 ± 0.3	0.353	4.987	0.622
LM-4	Becrock	Arkosic ss	285	48°23.7′	122°18.5′	540 ± 13	15.5 ± 0.4	0.336	5.651	0.580
Sample ID[d]	Sample type	Lithology	Altitude [m]	Latitude [°N]	Longitude [°W]	^{36}Cl/Cl (10^{-15})	^{36}Cl age $\pm 1\sigma$ (10^3 yr)	Thickness averaged production rates [atoms ^{36}Cl (g ∗ yr)$^{-1}$] ΨCa	ΨK	ΨN
ANDERSON-D	Erratic	Granodiorite	52	48°02.6′	122°30.2′	112 ± 21	12.2 ± 2.3 s.o.	2.640	2.207	3.059
SHAW-NES	Erratic	Graywacke	52	48°02.6′	122°30.2′	286 ± 32	13.9 ± 1.6	2.527	1.373	0.630
IMBURGIA-B	Erratic	Granodiorite	46	48°02.0′	122°28.9′	113 ± 15	9.8 ± 1.3 s.o	2.160	1.800	1.399
COUPE-1B	Erratic	Greenstone	34	48°12.7′	122°41.2′	93.4 ± 4.2	16.8 ± 0.7	3.858	1.173	3.973
COUPE-IC	Erratic	Greenstone	34	48°12.7′	122°41.2′	91.0 ± 3.0	16.3 ± 0.5	3.858	1.173	3.973
LONG-C	Erratic	Granite	91	47′56.5′	122°24.6′	94.1 ± 2.9	12.9 ± 0.4 s.o.	0.874	6.237	5.185
SILLS	Erratic	Granodiorite	41	47°58.3′	122°27.1′	548 ± 40	54.3 ± 3.9 s.o.	2.654	1.049	1.407
ELL-ROB-2	Erratic	Granodiorite	20	48°00.1′	122°29.5′	536.9 ± 8.6	47.3 ± 1.6 s.o.	2.848	1.637	1.353
DEC-QTZ(wr)	Bedrock	Quartzite	57	48°24.0′	122°38.7′	474 ± 40	27.3 ± 2.3 s.o.	3.931	0.535	0.661
ELL-ROB-1	Erratic	Basalt	20	48°00.1′	122°29.5′	119 ± 10	9.2 ± 0.8 s.o.	7.253	0.781	2.136
TARA-1B(94)	Erratic	Greenstone	21	48°00.5′	122°33.5′	133 ± 7.8	13.1 ± 0.8	12.923	0.018	3.923
ROSCHT-4	Bedrock	Chert	25	48°25.0′	122°40.0′	126 ± 8.1	16.8 ± 1.0	0.019	0.918	0.752
ROSCHT-5	Bedrock	Chert	25	48°25.0′	122°40.0′	217 ± 6.1	23.1 ± 0.6 s.o.	0.214	1.340	0.637

[a] Samples used to solve ^{36}Cl production rate due to neutron activation of ^{35}Cl. SERHAR and CLINTON samples high water content (10–12 wt.%).

[b] Samples used to solve ^{36}Cl production rate due to spallation of calcium.

[c] Samples used to solve ^{36}Cl production rate due to spallation of potassium.

[d] Samples that were not used to calibrate ^{36}C1 production rates. These samples were not used for one of the following reasons: 1. large accelerator mass spectrometry analytical uncertainties; 2. inappropriate isotopic chemistry; 3. determined to be statistical outliers (s.o.) where the mean age is $>3\sigma$ from the calibration age (15,500 yr).

Individual ground-level secondary neutron production rate in air [$P_f(0)$] values inferred from thermal neutron absorption by ^{35}Cl (Table 3 and Fig. 5) show a bimodal distribution. This suggests that the thermal neutron absorption rate likely is about 40% greater for samples with high water content (i.e., serpentinized samples) compared with samples with relatively low water content. The calculated $P_f(0)$ in air, inferred from thermal neutron absorption by ^{35}Cl, is 762 ± 28 neutrons (g air)$^{-1}$ yr^{-1} for samples with low water content (1–2 wt.%). The calculated $P_f(0)$ inferred from thermal neutron absorption by ^{35}Cl

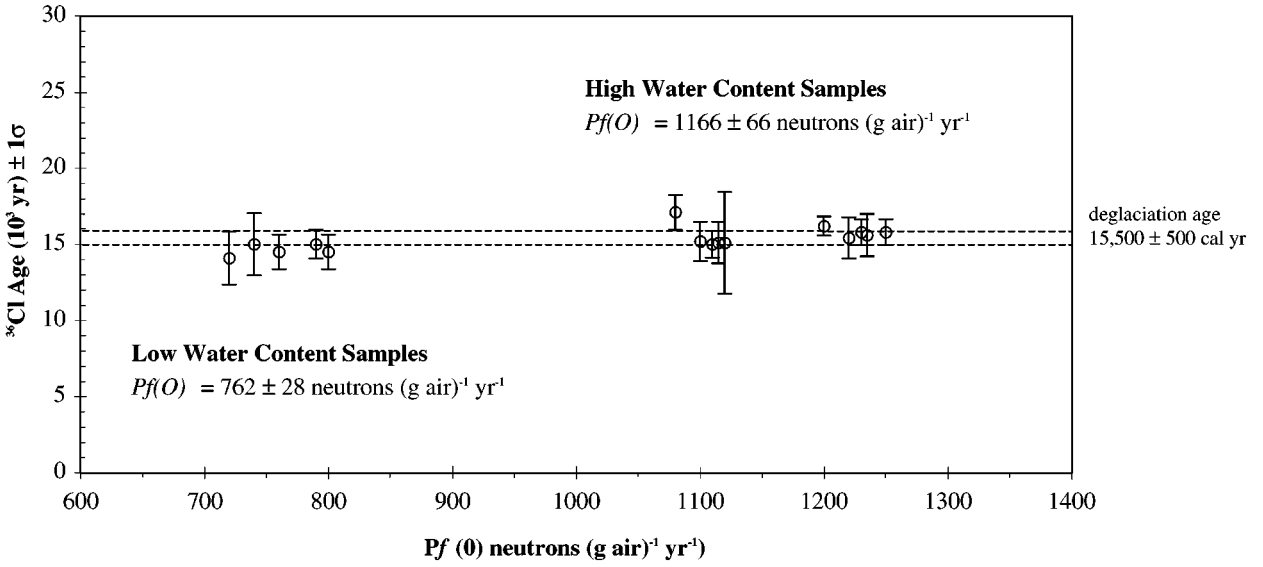

FIG. 5. Individual ground-level secondary neutron production rate $P_f(0)$ values inferred from thermal neutron absorption by ^{35}Cl show a bimodal distribution suggesting that the thermal neutron absorption rate is at least ~40% greater for the samples possessing high water content (serpentinized samples) compared with those samples possessing relatively low water content. The calculated mean secondary neutron production rate in air [$P_f(0)$] $\pm 1\sigma$ error for the low water calibration samples is 762 ± 28 fast neutrons (g air)$^{-1}$ yr^{-1}.

using high water content (10–12 wt.%) samples is 1166 ± 66 neutrons (g air)$^{-1}$ yr^{-1}. The inconsistency between the inferred ground-level secondary neutron production rate of the low versus high water content samples suggests that existing models do not adequately describe thermalization and capture of neutrons for hydrous rock samples. If the neutron thermalization model of Liu *et al.* (1994) were applicable to samples with such high water contents as the harzburgites, we would expect to obtain a single value (or tight group of values) of $P_f(0)$ estimates from all samples. Instead, there is a bimodal distribution, which suggests that the thermal neutron absorption rate is greater for hydrous samples. The bimodal distribution is qualitatively consistent with the model findings of Dep *et al.* (1994), which predicted that the relative thermal neutron flux increases nonlinearly as water content increases. Consequently, future ^{36}Cl age calculations for hydrous rock samples in which thermal neutron absorption by ^{35}Cl is an important production pathway will require a more detailed model if neutron thermalization and capture are to be described accurately. A study by Phillips *et al.* (2001) may remedy this problem regarding water-rich samples. Our $P_f(0)$ value for more common samples, with water content <2%, is 762 ± 28 neutrons (g air)$^{-1}$ yr^{-1}.

The total production rate due to calcium (Ψ_{Ca}) was calculated using 11 calibration samples with high Ca/Cl and Ca/K ratios (i.e., basalts, gabbros, mafic metavolcanics; Table A1 in Appendix). Only those samples for which calcium reactions contributed 65–90% of the total ^{36}Cl production were used to solve for Ψ_{Ca} (Table 3). To estimate the ^{36}Cl production rate from Ca in these samples, the neutron-produced fraction was calculated and subtracted using the above value [762 ± 28 neutrons (g air)$^{-1}$ yr^{-1}]. Potassium production is negligible in these samples. The production rate of the remaining ^{36}Cl due to reactions on Ca is 91 ± 5 atoms ^{36}Cl (g Ca)$^{-1}$ yr^{-1} (Table A1 in Appendix and Fig. 6). The production rate of ^{36}Cl due solely to calcium spallation can be estimated from this total value by subtracting the rate of muon capture [$^{40}Ca(\mu,\alpha)\,^{36}Cl$] obtained by Stone *et al.* (1998) of $\sim 5 \pm 2$ atoms (g Ca)$^{-1}$ yr^{-1}. The production rate due to spallation of Ca is $\sim 86 \pm 5$ atoms ^{36}Cl (g Ca)$^{-1}$ yr^{-1}.

The total production rate due to potassium (Ψ_K) was calculated using eight calibration samples that possess relatively high K/Cl and K/Ca ratios (i.e., felsic and intermediate plutonic rocks and arkosic sandstones; Table A1 in Appendix). Samples for which production due to potassium contributed to 38–85% of the total ^{36}Cl production were used to solve for Ψ_K (Table 3). To estimate Ψ_K in these samples, contributions from neutron capture and reactions on Ca were calculated using the values of $P_f(0)$ and Ψ_{Ca} derived above and subtracted. The calculated production rate for potassium is 228 ± 18 atoms ^{36}Cl (g K)$^{-1}$ yr^{-1} (Table 3 and Fig. 7).

The quoted uncertainties represent the standard error about the mean. Among other sources of uncertainty, several may be significant (e.g., uncertainty in the AMS measurement, which is generally less than 5%, and the error associated with the ^{35}Cl determination). The measurement errors are within the bounds expressed by the above uncertainty. More realistic uncertainties must also consider other factors, especially those related to geochemical effects on neutron transport and the overall geologic context of the individual samples. Our quoted uncertainties do not consider systematic uncertainties from these two sources.

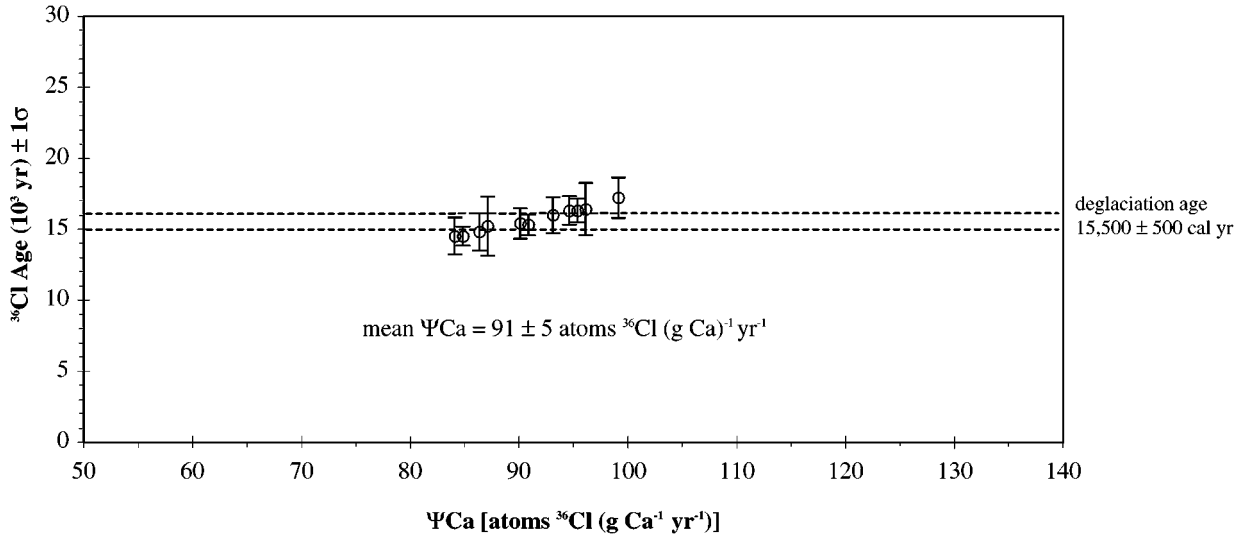

FIG. 6. The calculated mean $\pm 1\sigma$ error for the production rate due to calcium (P_{Ca}) is 91 ± 5 atoms ^{36}Cl (g Ca)$^{-1}$ yr^{-1}.

Internal Consistency and Validity of ^{36}Cl Production Rates

To assess internal the consistency of the sample population, ^{36}Cl ages were calculated for all samples using the new production rates (Fig. 8). The calculated mean ^{36}Cl age ($\pm 1\sigma$) for the individual sample ages is 15,700 ± 800 ^{36}Cl yr. The ±5.1% mean standard deviation of the sample population likely represents a minimum estimation of the statistical variability due to uncertainties within production rate parameters. The calculated mean and standard deviation excludes samples with ages more than 3σ outside the combined mean.

The large discrepancy between the mean ^{36}Cl age of the calibration samples and that of the statistical outliers (Fig. 8) most likely reflects geologic or anthropogenic factors, including prior exposure history (Briner and Swanson, 1998), surface degradation and/or spalling of boulders due to natural weathering effects or fire (Bierman and Gillespie, 1991), and post-depositional reorientation of boulders (e.g., during farming and logging operations or major seismic events).

To test the validity of the derived production rates, ^{36}Cl ages were calculated for rock samples collected from the surface of a dacite flow erupted in the Garibaldi volcanic region, British Columbia, and glacially abraded bedrock and erratics at three localities deglaciated transgressively over a 7000- to 8000-yr interval (Fig. 9). The Ring Creek dacite flow was erupted shortly after deglaciation of Howe Sound, British Columbia (12,600–10,800 cal yr B.P.), based on bracketing ^{14}C ages of wood underlying and overlying the flow (Brooks and Friele, 1992). The Cordilleran Ice Sheet retreated from its southernmost limit in the southern Puget Lowland 17,000–16,700 cal yr ago (Porter

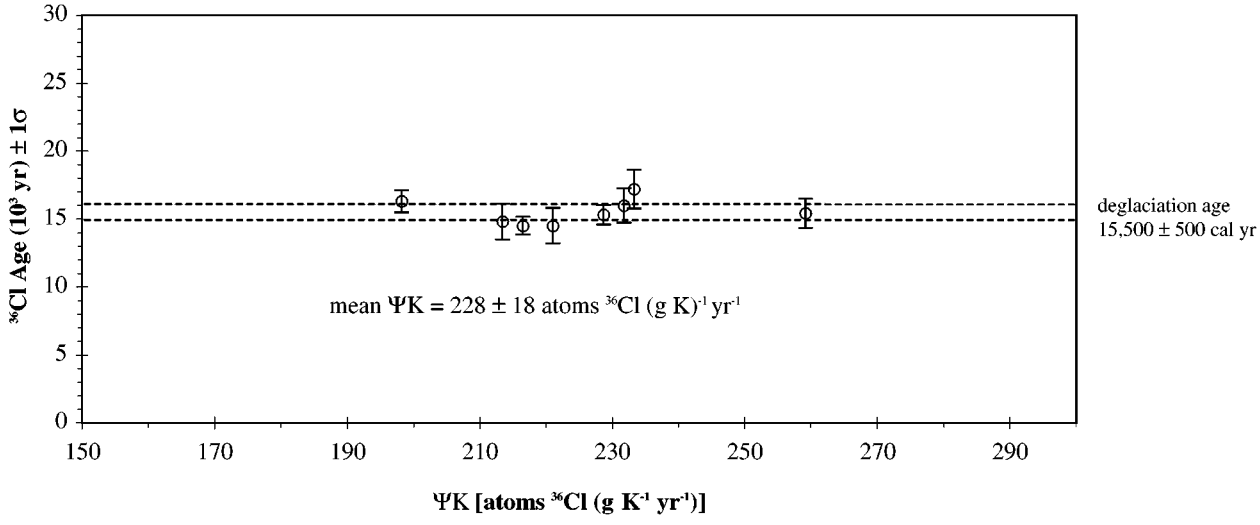

FIG. 7. The calculated mean $\pm 1\sigma$ error for the production rate due to (P_K) is 228 ± 18 atoms ^{36}Cl (g K)$^{-1}$ yr^{-1}.

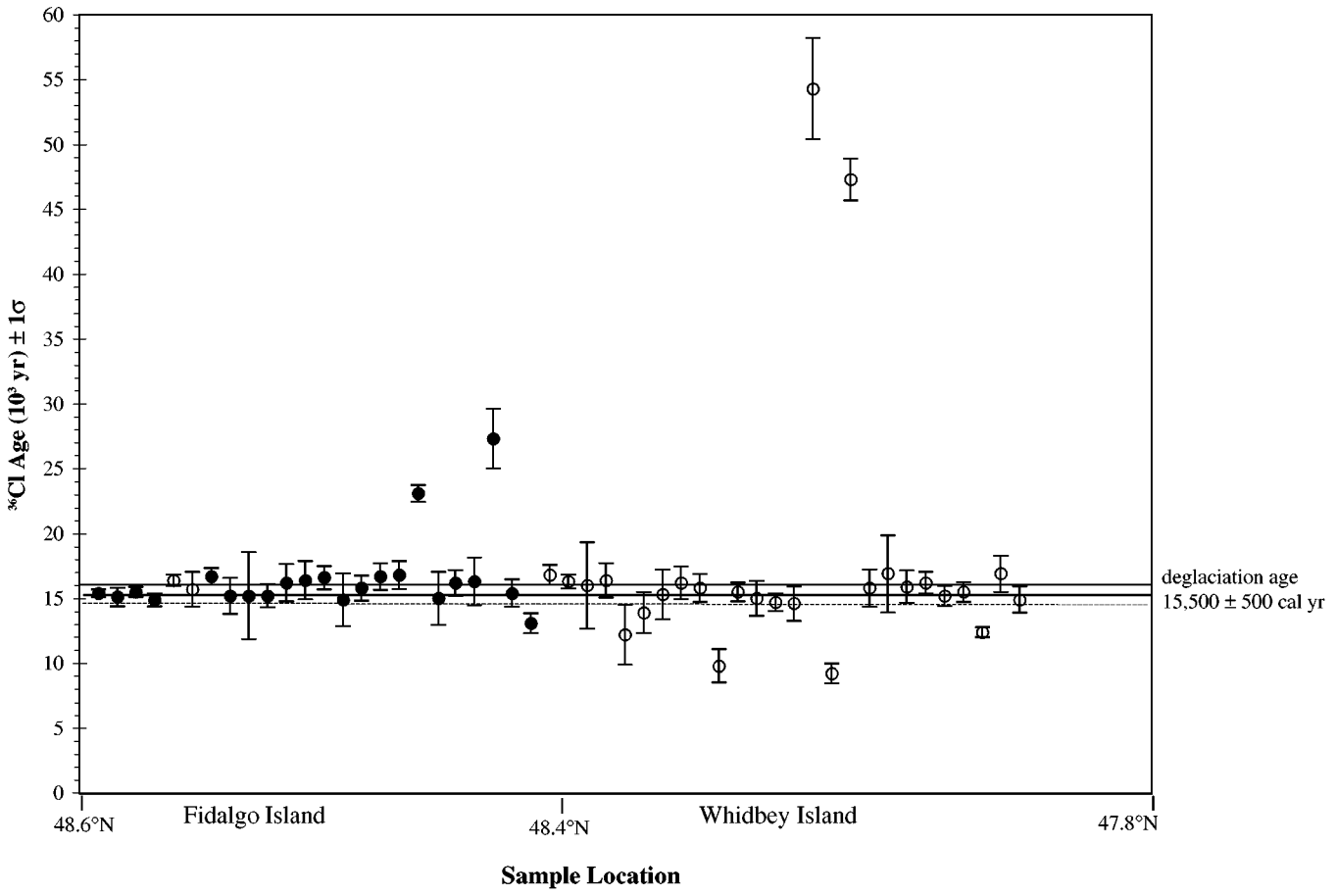

FIG. 8. Distribution of ^{36}Cl ages for all samples collected from Whidbey and Fidalgo Islands using the derived production rates. Statistical outliers are included and are also listed in the lower section of Table 3 and designated with the letters "s.o." Bedrock and erratic boulder samples are shown as filled and open circles, respectively.

and Swanson, 1998) and stabilized or readvanced in the Fraser Valley, British Columbia, 13,500–12,500 cal yr ago (Clague *et al.*, 1997). East of the Cascade Range, the ice margin retreated from its maximum limit on the Waterville Plateau before ~17,000 cal yr ago (Atwater, 1986). Remnant ice melted from the interior plateau of British Columbia before 9700 cal yr ago (Clague, 1981).

^{36}Cl ages and geographic and geochemical data are shown in Table 4 and Table A2 of the Appendix. The mean ^{36}Cl ages $\pm 1\sigma$ for the Ring Creek lava flow, Vashon, Sumas, and interior British Columbia samples are 11,600 ± 600, 18,800 ± 2,000, 13,700 ± 1,800, and 10,400 ± 500 ^{36}Cl yr, respectively, which are consistent with the calibrated radiocarbon ages for these sites (Fig. 10). The close agreement between the calculated ^{36}Cl ages and independent ^{14}C ages for these supports the reliability of the newly derived ^{36}Cl production rates. The uncertainty for each of the three groups likely reflects analytical uncertainties related to the ^{36}Cl age solutions and geological factors.

Our production rates were also used to calculate ^{36}Cl ages of moraines of the last glaciation in the Ahklun Mountains, southwestern Alaska (Briner *et al.*, in press). The resulting chronology is consistent with ^{14}C and thermoluminescence ages related to glaciation in this region. Briner *et al.* (in press) reported that ^{36}Cl ages calculated using other published ^{36}Cl production rates yield ages that are inconsistent with the independent ^{14}C and thermoluminescence ages.

Comparison with other production rate estimates. Several other studies have derived ^{36}Cl production rates based on empirical calibrations (Zreda *et al.*, 1991; Phillips *et al.*, 1996; Stone *et al.*, 1996; Evans *et al.*, 1997). To compare these production rates with our rates, all have been scaled to sea level and high latitude using the scaling parameters of Lal (1991), i.e., to essentially the same geographic latitude and altitude as samples used for calibration in this study (Table 1).

Our calculated $P_f(0)$ [762 ± 28 fast neutrons (g air)$^{-1}$ yr^{-1}] is consistent with measured neutron flux values of 10^{-3} to 2×10^{-3} n cm^{-1} s^{-1} (Simpson, 1951; Hendrick and Edge, 1966; Yamashita *et al.*, 1966), which are equivalent to capture-rate values of 2 to 4×10^5 neutrons (kg rock)$^{-1}$ yr^{-1}. Our calculated ground-level secondary neutron production rate is about 35%

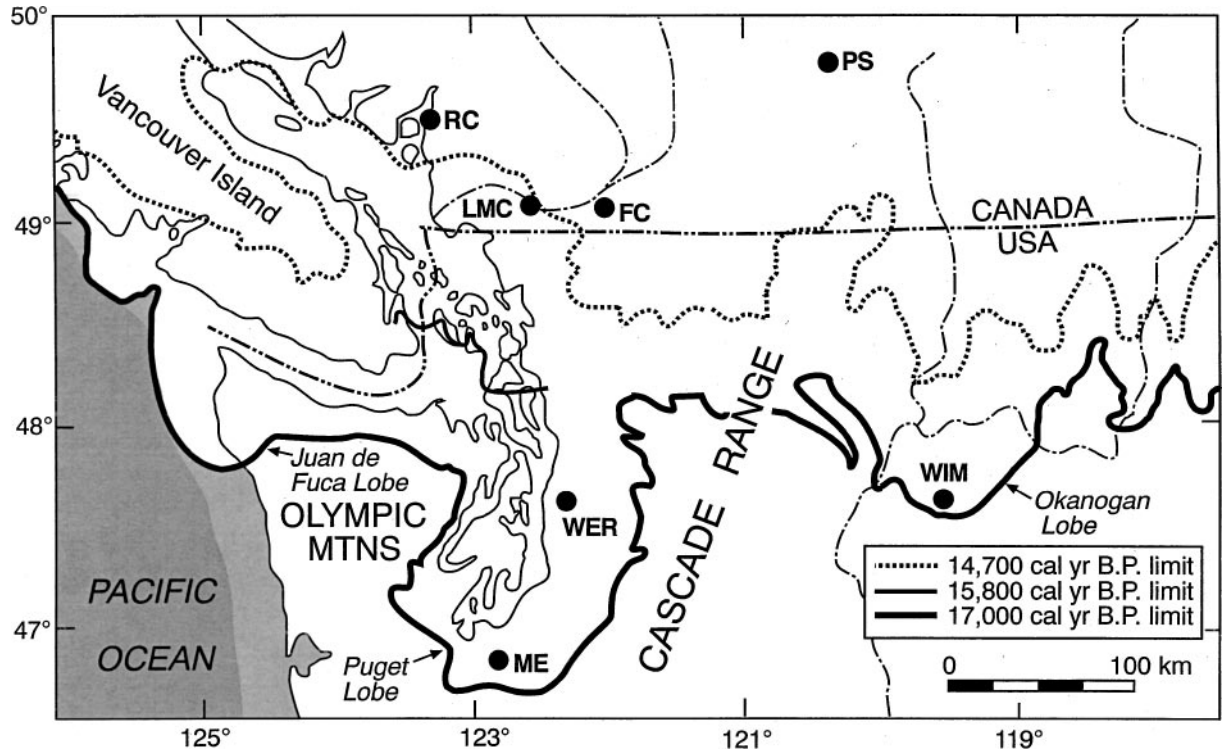

FIG. 9. Map showing the terminal position of the Cordilleran Ice Sheet at different times during the recessional phase of the Fraser Glaciation. Ice limit reconstructions taken from Clague *et al.* (1988) and Porter and Swanson (1998). Light-gray shading shows the inferred last glaciation emerged coast line. Location of the sample sites (including Ring Creek dacite flow) used to test the validity of the ^{36}Cl production rates are designated by their respective sample abbreviations.

greater than the experimentally calculated value of 586 ± 40 obtained by Phillips *et al.* (1996).

Whereas spallation reactions with Ca typically account for 80–90% of ^{36}Cl production in calcium-bearing minerals, negative muon capture becomes increasingly important near sea level and at depth. To compare Ca production rates, it is necessary to use values that represent total production from Ca production rates calculated by Phillips *et al.* (1996) and in this study did not isolate the muon production rate. Stone *et al.* (1998) estimated a surface production rate of $\sim 5 \pm 2$ atoms (g Ca)$^{-1}$ a^{-1} for the muon capture reaction [^{40}Ca(μ,α)^{36}Cl] at high latitude and at sea level, which must be added to Stone *et al.*'s (1996) production rate due to spallation of Ca (48.8 ± 1.7 atoms ^{36}Cl g Ca^{-1} yr^{-1}). Our total ^{36}Cl production rate from Ca (91 ± 5 atoms ^{36}Cl g Ca^{-1} yr^{-1}) is about 20% greater than that calculated experimentally by Zreda (1994) and Phillips *et al.* (1996) and about 60% greater than the value obtained by Stone *et al.* (1996) (Table 1).

Production rates from potassium have been reported in several studies using potassium-rich rocks or minerals (Zreda *et al.*, 1991; Zreda, 1994; Phillips *et al.*, 1996; Evans *et al.*, 1997) (Table 1). Although three independent potassium reactions produce cosmogenic ^{36}Cl, high-energy spallation reactions predominate at the surface, whereas negative muon capture and thermal neutron capture of ^{39}K are minor surface reactions. The values reported in Table 1 represent the total surface production rate of ^{36}Cl from potassium reactions.

Our potassium production rate, 228 ± 18 atoms ^{36}Cl g K^{-1} yr^{-1}, is higher than the scaled values reported by Zreda (1994) and Phillips *et al.* (1996) by $\sim$10% and 35%, respectively. Evans *et al.* (1997) reported two different production-rate values for potassium: 170 ± 25 atoms ^{36}Cl g K^{-1} yr^{-1} averaged for Sierra Nevada and Scottish samples and 241 ± 9 atoms ^{36}Cl g K^{-1} yr^{-1} for two Antarctic bedrock samples. Evans *et al.* (1997) stated that the differences between the two production-rate values are real and cannot be attributed to meteoric ^{36}Cl. They postulated that either the production rate differs over 10^4- to 10^6-yr time scales or that the altitude scaling applied to Antarctica underestimates the true scaling factor for the Antarctic atmosphere.

Possible Causes of Inconsistency between ^{36}Cl Production Rates

The discrepancy between various production-rate values is likely due to a combination of factors. Although no consistent pattern of variance is seen between each respective research group's production rates, several hypotheses can be advanced to explain these discrepancies.

Prior exposure (inheritance) effects on ^{36}Cl production. Anomalously old exposure ages may result from ^{36}Cl inherited from exposure prior to the last glaciation (Briner and Swanson, 1998). The geologic setting and the similarity in exposure ages of most of the samples collected close to the calibration samples make this explanation unlikely. Almost all erratic boulders

TABLE 4
Lithology, Location, Altitude, ^{36}Cl Ratios, ^{36}Cl and ^{14}C Ages for Samples Used to Test the Validity of the ^{36}Cl Production Rates

Sample ID[a]	Sample type	Lithology	Altitude [m]	Latitude [°N]	Longitude [°W]	^{36}Cl/Cl (10^{-15})	^{36}Cl AGE ± 1σ (10^3 yr)	^{14}C Age (10^3 cal yr)
ME-2A	Erratic	Granodiorite	157	46°50.5′	122°38.0′	180 ± 5.9	16.4 ± 0.6	~17–18
ME-2	Erratic	Granodiorite	157	46°50.5′	122°38.0′	236 ± 23	19.8 ± 1.9	~17–18
ME-3	Erratic	Granodiorite	157	46°50.5′	122°38.0′	273 ± 26	20.0 ± 1.8	~17–18
WER-1	Erratic	Greenstone	97	47°41.0′	122°41.5′	687 ± 36	15.3 ± 0.7	~16–17
WIM-BAS	Erratic	Basalt	780	47°45.0′	119°45.0′	232 ± 7.2	18.1 ± 0.6	>16.5
WIM5BT	Erratic	Basalt	780	47°45.0′	119°45.0′	248 ± 13	19.7 ± 1.1	>16.5
WIM1BF	Erratic	Granite	780	47°45.0′	119°45.0′	381 ± 7.6	18.1 ± 0.4	>16.5
WIM4F	Erratic	Granite	780	47°45.0′	119°45.0′	483 ± 40	21.2 ± 1.8	>16.5
WIM-1	Erratic	Granite	780	47°45.0′	119°45.0′	504 ± 9.0	19.3 ± 0.3	>16.5
WIM4B	Erratic	Gneiss	780	47°45.0′	119°45.0′	610 ± 59	22.1 ± 2.1	>16.5
Sample ID[b]	Sample type	Lithology	Altitude [m]	Latitude [°N]	Longitude [°W]	^{36}Cl/Cl (10^{-15})	^{36}Cl AGE ± 1σ (10^3 yr)	^{14}C Age (10^3 cal yr)
LMC-1	Bedrock	Argillite	100	49°11.5′	121°54.0′	117 ± 10	13.2 ± 1.1	12.5–13.5
LMC-2	Bedrock	Argillite	100	49°11.5′	121°54.0′	87.8 ± 5.9	13.9 ± 0.9	12.5–13.5
LMC-3	Bedrock	Argillite	100	49°11.5′	121°54.0′	103 ± 9	16.7 ± 1.5	12.5–13.5
FC-1	Bedrock	Conglomerate	90	49°22.5′	121°33.0′	158 ± 3.0	12.8 ± 0.2	12.5–13.5
FC-1B	Bedrock	Conglomerate	90	49°22.5′	121°33.0′	147 ± 7.2	11.9 ± 0.6	12.5–13.5
Sample ID[c]	Sample type	Lithology	Altitude [m]	Latitude [°N]	Longitude [°W]	^{36}Cl/Cl (10^{-15})	^{36}Cl AGE ± 1σ (10^3 yr)	^{14}C Age (10^3 cal yr)
PS-1	Bedrock	Granodiorite	1728	49°54.0′	120°02.5′	392 ± 9.6	10.7 ± 0.3	>9.7
PS-2	Bedrock	Granodiorite	1728	49°54.0′	120°02.5′	368 ± 17	10.0 ± 0.5	>9.7
PS-3	Bedrock	Granodiorite	1728	49°54.0′	120°02.5′	274 ± 9.1	10.6 ± 0.3	>9.7
PS-4	Bedrock	Granodiorite	1728	49°54.0′	120°02.5′	372 ± 13	10.7 ± 0.4	>9.7
PS-5	Bedrock	Granodiorite	1728	49°54.0′	120°02.5′	384 ± 13	10.7 ± 0.4	>9.7
Sample ID[d]	Sample type	Lithology	Altitude [m]	Latitude [°N]	Longitude [°W]	^{36}Cl/Cl (10^{-15})	^{36}Cl AGE ± 1σ (10^3 yr)	^{14}C Age (10^3 cal yr)
RING CK-1	Bedrock	Dacite	290	49°43.3′	123°03.2′	55 ± 3.5	11.6 ± 0.7	10.8–12.6
RING CK spk	Bedrock	Dacite	290	49°43.3′	123°03.2′	57 ± 3.7	11.9 ± 0.8	10.8–12.6

[a] Samples collected from deglaciated surfaces in the southern Puget Lowland and Waterville Plateau, Washington, inferred to be Vashon maximaum age.
[b] Samples collected from deglaciated surfaces in the Fraser Valley, British Columbia, inferred to be post-Sumas age.
[c] Samples collected from deglaciated surfaces in the Interior Plateau, British Columbia, inferred to be latest deglaciation.
[d] Samples collected from the Ring Creek dacite flow, near Squamish, British Columbia.

sampled for calibration were transported >75 km from likely bedrock sources. Supraglacial debris falling from exposed nunataks likely represent an insignificant fraction of Vashon-age boulders. Many large sampled till boulders are embedded in Vashon till, and their long axes are aligned with the inferred ice-flow direction, implying subglacial transportation. Extensive proglacial outwash and lacustrine sediments that buried much of the pre-Vashon surface reduced the likelihood that rocks with prior exposure would be deposited in Vashon till.

Prior exposure effects due to muon production over multiple glacial cycles (i.e., 10^5 yr) may also result in higher ^{36}Cl/Cl ratios than the deglaciation age would permit, assuming glacial erosion rates are low in the glacier's accumulation area. Prior exposure effects resulting from long exposure to muons would be greatest for the Ca-rich samples. Consistent ages for the Ring Creek flow calculated using our Ca production rate suggest that prior exposure effects due to muon production is not a significant factor.

Temporal variability of the Earth's magnetic field. The production rates of Phillips *et al.* (1996) are based on calibration samples from 19°–70°N latitude [i.e., Hawaiian Islands, Craters of the Moon National Monument (Idaho), Great Britain, and Ellesmere Island (Canada)]. The strength of the Earth's magnetic field differs between low and high latitudes (Simpson, 1951), has varied by as much as ±30% over the past 100,000 yr (Reedy *et al.*, 1983), and experienced even greater variability over brief geologic time intervals during the last glaciation (Raisbeck *et al.*, 1987; Baumgartner *et al.*, 1998). This varying attenuation affects the intensity of cosmic radiation reaching the surface at different latitudes.

The production rates of Phillips *et al.* (1996) are based on samples from wide ranges of latitude and altitude. Furthermore,

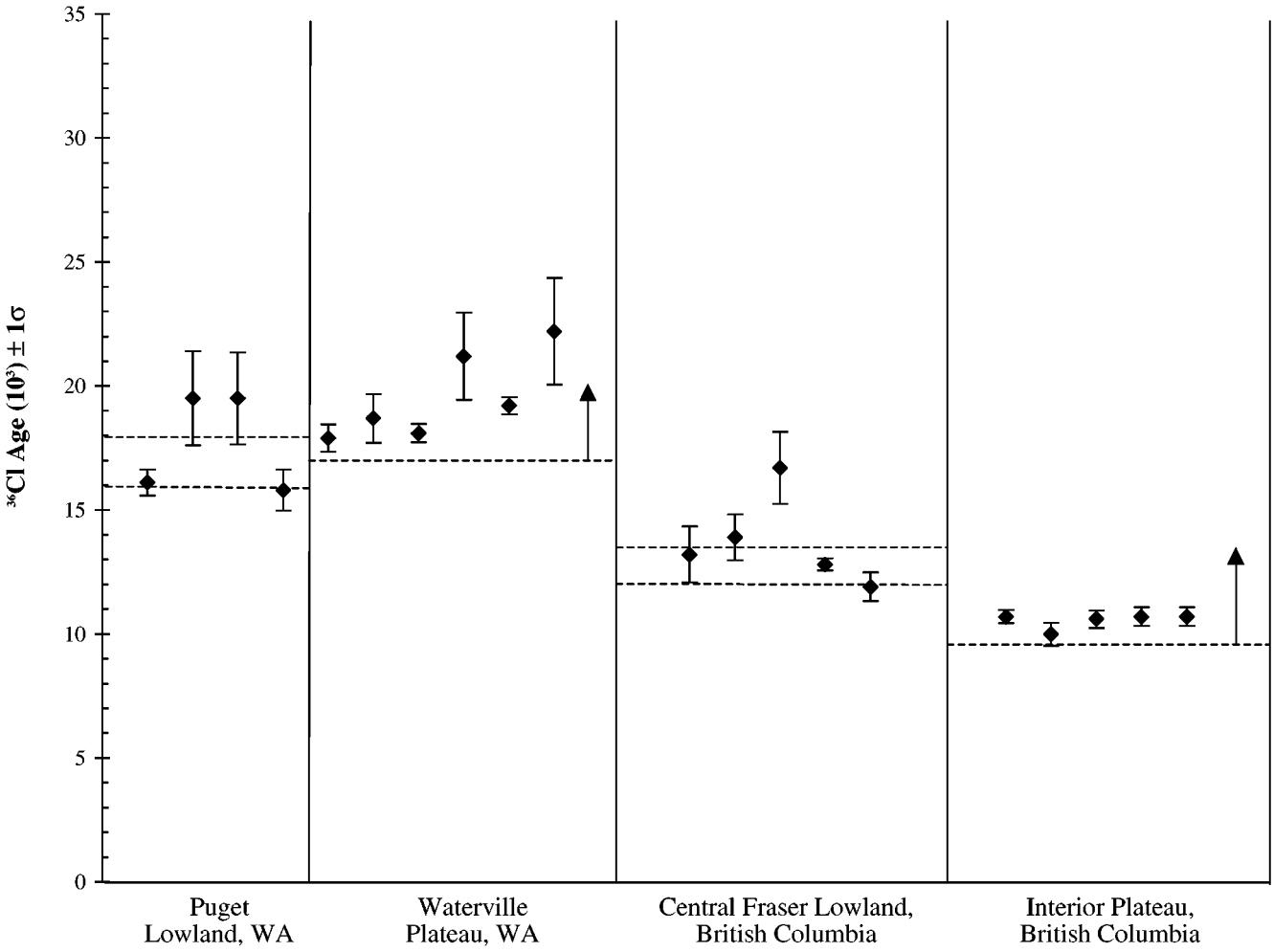

FIG. 10. Distribution of ^{36}Cl ages grouped according to their respective locations within the recessional limits of the Cordilleran Ice Sheet. The ^{36}Cl ages are consistent with independent radiocarbon ages constraining the timing of deglaciation at each location (bracketing calibrated ^{14}C ages are shown as two dashed lines; minimum limiting ages are shown as a single dashed line and arrow), supporting the validity of the production rates reported here. These data are further supported by the consistency of the calculated ^{36}Cl exposure age, using our production rates, and ^{14}C constraints for the eruption of Ring Creek dacite flow near Squamish, British Columbia (discussed in text).

independent calibration ages range between 3000 (^{14}C-bracketed basalt flows [Craters of the Moon, Idaho]) and 55,000 yr (K/Ar-dated Hawaiian basalt flows). Average production rate solutions integrated over this time interval likely do not equal the average production rates of the last 15,500 cal yr (Meynadier *et al.*, 1992; Tric *et al.*, 1992). Moreover, Clark *et al.* (1995) reported that field-strength-induced changes in cosmogenic nuclide production rates are greatest at low latitudes and high altitudes. The calibration samples used in this study were collected in a limited geographic area (47.5–48°N latitude), near sea level, and reflect the average production rate over the last 15,500 ^{36}Cl yr. Correcting for magnetic field intensity changes for our calibration latitude and exposure age (i.e., geographic latitude of 47.4° vs effective latitude of 48.2°) would change our calculated production rates by <2%.

Error in Latitude–Altitude Scaling Factors. Three reported scaling curves correct for latitude–altitude variation in the neutron flux (i.e., Yokoyama *et al.*, 1977; O'Brien, 1979; Lal, 1991). Our study, as well as others (Table 1), used the latitude–altitude curves of Lal (1991) to scale the production rates to high-latitude and sea-level conditions. Of the three scaling curves, Lal's (1991) is the only one based on experimentally measured neutron flux rates in the atmosphere. It is unlikely that altitude scaling is responsible for much of the discrepancy between our production rates and those of others (i.e., Phillips *et al.*, 1996; Stone *et al.*, 1996; Evans *et al.*, 1997), as ^{36}Cl ratios measured for Hawaiian basalt flows were consistent with theorized values based on Lal's (1991) altitude scaling curves (Zreda *et al.*, 1991). Furthermore, ^{36}Cl ages calculated for deglaciation of the Waterville Plateau (~750 m) using the Whidbey Island

production parameters are reasonable and are consistent with minimum ^{14}C ages of sediments associated with the draining of glacial Lake Columbia during retreat of the Okanogan Lobe (Atwater, 1986).

An error in latitude scaling would affect all production pathways similarly. Therefore, ^{36}Cl ages based on one set of production parameters should be internally consistent, regardless of sample composition. Because ^{36}Cl production rates do not vary consistently between each research group's calibration sites, latitude scaling error is unlikely to be the principal cause of the discrepancy between the various production rates.

Surface erosion effects on ^{36}Cl production. Surface weathering and fire-induced spalling can present problems if single cosmogenic isotopes are used to date geomorphic surfaces (e.g., Bierman and Gillespie, 1991). However, the data presented in Figure 8 indicate that these two factors alone are not a serious problem for dating late Pleistocene surfaces in western Washington. Glacial striations, grooves, and raised quartz veins are seen on some exposed bedrock surfaces and erratic boulders and limit average surface erosion over the last 15,500 ^{36}Cl yr: <1 cm (relief of quartz vein) from the surface of coarse-grained lithologies (Fig. 4) and <5 mm (depth of striations) from fine-grained metamorphic lithologies (Fig. 3). Erosion rates of <0.03 to 0.26 cm $(10^3\ \text{yr})^{-1}$ are therefore implied for these fine- and coarse-grained lithologies, respectively. Rates of this magnitude are of little consequence for obtaining accurate exposure ages for surfaces dating to the last glaciation.

The effect of fire on measured $^{36}Cl/Cl$ ratios was qualitatively evaluated by comparing individual ^{36}Cl production-rate solutions of drift boulders and abraded bedrock sites still possessing striations with boulders exhibiting spalled surfaces. Production-rate solutions are consistent between the two subgroups; thus, it can be inferred that spalling due to forest fires is not a major problem for the calibration boulders used in this study (Fig. 8).

Of the calibrated production pathways, production of ^{36}Cl by neutron absorption is most sensitive to geologic factors, such as erosion rate. Whereas erosion rates can be estimated for surfaces retaining glacial abrasion features or with differentially eroded quartz veins, the coarse-grained rock samples in our study (e.g., plutonic and coarse clastic sedimentary) did not possess small-scale glacial abrasion features; consequently, erosion rate estimates for this surface have greater uncertainty.

Poorly constrained calibration ages. A possible reason for the inconsistency between the different production rates is poorly constrained ages for calibration surfaces. The exposure age (deglaciation age) of our Puget Sound calibration area is controlled by numerous calibrated ^{14}C ages that date the time of deglaciation. Porter and Swanson (1998) provided a detailed calibrated ^{14}C chronology for the advance and retreat history of the Puget Lobe 30 to 100 km south of the calibration sites used in this study. The ^{14}C age constraints they discussed are based solely on wood and gyttja samples but are consistent with the glacialmarine shell ages used by Swanson (1994) to constrain the deglaciation history of the Whidbey and Fidalgo Islands.

For many of the numerical ages used by Phillips *et al.* (1996) to calibrate their production rates, the relationship between the limiting age and the related surface is uncertain; in some instances the error range is large. For example, the K/Ar date of 55,000 yr B.P. for the Hawaiian lava flow has an analytical uncertainty of $\pm 12\%$. Some of the limiting radiocarbon ages for basalt flows in Craters of the Moon National Monument used as calibration samples are based on bulk samples of underlying soils. A potential problem with bulk soil ages is that the organic content in soils can take 10^2–10^3 yr to reach equilibrium (Birkeland, 1984). Such uncertainties may contribute to some of the observed inconsistencies in the production rates.

Stone *et al.* (1996) used the Tabernacle Hill basalt flow in Utah to calibrate the production rate due to calcium. This flow was erupted onto the Provo shoreline of Lake Bonneville and its age is believed to be $14{,}400 \pm 100$ ^{14}C yr B.P. (Oviatt and Nash, 1989; $\sim 17{,}300 \pm 300$ cal yr B.P., Stuiver and Reimer, 1993). It is difficult to reconcile the difference in calcium production rates of Stone *et al.* (1996) (53.6 ± 1.8 atoms $^{36}Cl\ g\ Ca^{-1}\ yr^{-1}$) and those reported here (91 ± 5 atoms $^{36}Cl\ g\ Ca^{-1}\ yr^{-1}$), for both calibration sites appear to have reasonable dating control and inferred erosion rates.

The two K production rate values reported by Evans *et al.* (1997) are based on samples from three different sites. The lower potassium production rate (170 ± 25 atoms $^{36}Cl\ g\ K^{-1}\ yr^{-1}$) was determined using K-feldspar from ice-scoured bedrock in the eastern Sierra Nevada, California, and at Loch Lomond, Scotland. Neither calibration surface has been directly dated. The earliest deglaciation age ($11{,}190 \pm 70$ ^{14}C yr B.P., CAMS-11382; $\sim 13{,}100$ cal yr B.P.) from the eastern Sierra Nevada used for calibration is based on a single bulk ^{14}C age of gyttja collected from a tarn upstream from Recess Peak moraines (Clark and Gillespie, 1997). Samples from such sites provide only minimum limiting ages for deglaciation and conceivably postdate ice withdrawal by 10^2–10^3 yr.

Poorly constrained dating control of calibration samples may not explain all the inconsistency between the different production rates. More likely, a combination of several factors explains the differences shown in Table 1. An additional factor is the difference in chemical extraction procedures used by each research group. Swanson, Zreda, and Phillips used whole-rock chemical extraction procedures in their respective calibrations, whereas Stone and Evans used mineral separates. If the behavior of Cl varies with the extraction processes, differences in $^{36}Cl/Cl$ ratios could result, thereby influencing production rate calculations. Although it is not obvious how differences in the extraction process would translate to differences in production rates, this factor can easily be tested by having each research group extract and process Cl from the same sample subset.

ACKNOWLEDGMENTS

We thank J. Southon and R. Finkel for assistance with AMS measurements; D. Mohler and J. Briner for laboratory assistance; A. Gillespie, F. Phillips, S. C. Porter, J. Stone, M. Stuiver, and two anonymous reviewers for reading early and revised drafts of this paper; and the residents of Whidbey Island for allowing us to sample till boulders on their property. Swanson also thanks F. Phillips and M. Zreda for their openness in sharing their expertise and laboratory during the early stages of development of this research. This project was supported by the National Science Foundation (Grant ATM-9009104).

REFERENCES

Anundsen, K., Abella, S., Leopold, E., Stuiver, M., Turner, S. (1994). Late-glacial and early sea-level fluctuations in the central Puget Lowland, Washington, inferred from lake sediments. *Quaternary Research* **42,** 149–161.

Aruscavage, P. J., and Campbell, E. Y. (1983). An ion-selective electrode method for determination of chlorine in geological materials. *Talanta* **28,** 745–749.

Atwater, B. F. (1986). Pleistocene glacial-lake deposits of the Sanpoil River valley, northeastern Washington. *U.S. Geological Survey Bulletin 1661*.

Bard, E., Arnold, M., Fairbanks, R. G., and Hamelin, B. (1993). 230Th-234U ages obtained by mass spectrometry on corals. *Radiocarbon* **35,** 215–230.

Baumgartner, S., Beer, J., Masarik, J., Wagner, G., Meynadier, L., and Synal, H.-A. (1998). Geomagnetic modulation of the ^{36}Cl flux in the GRIP ice core, Greenland. *Science* **279,** 1330–1332.

Bentley, H. W., Phillips, F. M., and Davis, S. N. (1986). Chlorine-36 in the terrestrial environment. *In* "Handbook of Environmental Isotope Geochemistry, Vol. 2, The Terrestrial Environment" (B. P. Fritz and J. C. Fontes, Eds.), pp. 422–480. Elsevier, New York.

Bierman, P., and Gillespie, A. (1991). Range fires: A significant factor in exposure-age determination and geomorphic evolution. *Geology* **19,** 641–644.

Birkeland, P. W. (1984). "Soils and Geomorphology." Oxford Univ. Press, New York.

Booth, D. B. (1991). Glacier physics of the Puget Lobe, southwest Cordilleran Ice Sheet. *Geographie Physique et Quaternaire* **45,** 301–315.

Brandon, M. T. (1989). Geology of the San Juan-Cascades nappes, northwestern Cascade Range and San Juan Islands. *In* "Geologic Guidebook for Washington and Adjacent Areas" (N. L. Joseph, Ed.). *Washington Division of Geology and Earth Resources Information Circular* **86,** 137–162.

Briner, J. P., and Swanson, T. W. (1998). Inherited cosmogenic ^{36}Cl constrains glacial erosion rates of the cordilleran ice sheet. *Geology* **58,** 3–6.

Briner, J. P., Swanson, T. W., and Caffee, M. L. (in press). Late Pleistocene cosmogenic ^{36}Cl chronology of the southwestern Ahklun Mountains, Alaska. *Quaternary Research*.

Brooks, G. R., and Friele, P. A. (1992). Bracketing ages for the formation of the Ring Creek lava flow, Garibaldi volcanic belt, southwestern British Columbia. *Canadian Journal of Earth Sciences* **29,** 2425–2428.

Bucknam, R. C., Hemphill-Haley, E., and Leopold, E. B. (1992). Abrupt uplift within the past 1700 yr at southern Puget Sound, Washington. *Science* **258,** 1611–1614.

Cerling, T. E., and Craig, H. (1994). Geomorphology and *in situ* cosmogenic isotopes. *Annual Review of Earth and Planetary Science* **22,** 273–317.

Clague, J. J. (1981). Late Quaternary geology and geochronology of British Columbia. Part 1: Radiocarbon dates. *Geologic Survey of Canada*, Paper 80–13.

Clague, J. J., Saunders, I. R., and Roberts, M. C. (1988). Ice-free conditions in southwestern British Columbia at 16,000 yr B.P. *Canadian Journal of Earth Sciences* **25,** 938–941.

Clague, J. J., Mathewes, R. W., Guilbault, J.-P., Hutchinson, I., Rickets, B. D. (1997). Pre-Younger Dryas resurgence of the southwestern margin of the Cordilleran Ice Sheet, British Columbia, Canada. *Boreas* **26,** 261–277.

Clark, D. H., and Gillespie, A. R. (1997). Timing and significance of Late-glacial and Holocene cirque glaciation in the Sierra Nevada, California. *Quaternary International* **38/39,** 21–38.

Clark, D. H., Bierman, P. R., and Larsen, P. (1995). Improving *in situ* cosmogenic chronometers. *Quaternary Research* **44,** 367–377.

Davis, J. C., Proctor, I. D., Southon, J. R., Caffee, M. W., Heikkinen, D. W., Roberts, M. L., Moore, T. L., Turtletaub, K. W., Nelson, D. E., Loyd, D. H., Vogel, J. S. (1990). LLNL/UC AMS facility and research programs. *Nuclear Instruments and Methods in Physics Research* **B52,** 269–272.

Dep, L., Elmore, D., Fabryka-Martin, J., Masarik, J., and Reedy, R. C. (1994). Production rate systematics of *in situ*-produced cosmogenic nuclides in terrestrial rocks: Monte Carlo approach of investigating ^{35}Cl(n, γ)^{36}Cl. *Nuclear Instruments and Methods in Physics Research B* **92,** 321–325.

Dethier, D. P., Pessel, Jr., F., Keuler, R. F., Balzarini, M. A., and Pevear, D. R. (1995). Late Wisconsinan glaciomarine deposition and isostatic rebound, northern Puget Lowland, Washington. *Geological Society of America Bulletin* **107,** 1288–1303.

Evans, J. M., Stone, J. O. H., Fifield, L. K., and Cresswell, R. G. (1997). Cosmogenic chlorine-36 production in K-feldspar. *Nuclear Instruments and Methods in Physics Research B* **123,** 334–340.

Fabryka-Martin, J. T. (1988). "Production of Radionuclides in the Earth and Their Hydrogeologic Significance, with Emphasis on Chlorine-36 and Iodine-129." Unpublished Ph.D. dissertation, University of Arizona.

Hendrick, L. D., and Edge, R. D. (1966). Cosmic ray neutrons near the Earth. *Physical Review* **145,** 1023–1025.

Kovanen, D. J., and Easterbrook, D. J. (2001). Late Pleistocene, post-Vashon, alpine glaciation of the Nooksack drainage, North Cascades, Washington. *GSA Bulletin* **113,** 274–288.

Lal, D. (1991). Cosmic ray labeling of erosion surfaces: *In situ* nuclide production rates and erosion models. *Earth and Planetary Science Letters* **104,** 424–439.

Leopold, E. B., Nickmann, R., Hedges, J. I., and Ertel, J. R. (1982). Pollen and lignin records of late Quaternary vegetation, Lake Washington. *Science* **218,** 1305–1307.

Liu, B., Phillips, F. M., Fabryka-Martin, J. T., Fowler, M. M., Biddle, R. S., and Stone, W. D. (1994). Cosmogenic ^{36}Cl accumulation in unstable landforms, I. Effects of the thermal neutron distribution. *Water Resources Research* **30,** 1071–1074.

Meynadier, L., Valet, J. P., Weeks, R., Shackleton, N. J., and Hagee, V. L. (1992). Relative geomagnetic intensity of the field during the last 140 ka. *Earth and Planetary Science Letters* **114,** 39–57.

Mullineaux, D. R., Waldron, H. H., and Rubin, M. (1965). Stratigraphy and chronology of late interglacial and early Vashon time in the Seattle area, Washington. *U.S. Geological Survey Bulletin* **1194-0,** 1–10.

O'Brien, K. (1979). Secular variations in the production of cosmogenic isotopes in the Earth's atmosphere. *Journal of Geophysical Research* **84**(A2), 423–431.

Oviatt, C. G., and Nash, W. P. (1989). Late Pleistocene basaltic ash and volcanic eruptions in the Bonneville Basin, Utah. *Geological Society of America Bulletin* **101,** 292–303.

Phillips, F. M., and Plummer, M. A. (1996). CHLOE: A program for interpreting *in situ* cosmogenic nuclide data for surface exposure dating and erosion studies. *Radiocarbon* **38,** 98.

Phillips, F. M., Leavy, B. D., Jannik, N. O., Elmore, D., and Kubik, P. W. (1986). The accumulation of cosmogenic-36 in rocks: A method for surface exposure dating. *Science* **231,** 41–43.

Phillips, F. M., Zreda, M. G., Flinsch, M. R., Elmore, D., and Sharma, P. (1996). A reevaluation of cosmogenic ^{36}Cl production rates in terrestrial rocks. *Geophysical Research Letters* **23,** 949–952.

Phillips, F. M., Stone, W. D., and Fabryka-Martin, J. T. (2001). An improved approach to calculating low-energy cosmic-ray neutron fluxes near the land/atmosphere interface. *Chemical Geology* **175,** 689–701.

Porter, S. C., and Swanson, T. W. (1998). Advance and retreat rate of the Cordilleran Ice Sheet in southeastern Puget Sound region. *Quaternary Research* **50,** 205–213.

Raisbeck, G. M., Yiou, F., Bourles, D., Lorius, C., Jouzel, J., and Barkov, N. I. (1987). Evidence for two intervals of enhanced ^{10}Be deposition in Antarctic ice during the last glacial period. *Nature* **326,** 825–826.

Rama, and Honda, M. (1961). Cosmic-ray-induced radioactivity in terrestrial materials. *Journal of Geophysics Research* **66,** 3533–3539.

Reedy, R. C., Arnold, J. R., and Lal, D. (1983). Cosmic ray record in solar system matter. *Science* **255,** 341–363.

Simpson, J. A. (1951). Neutrons produced in the atmosphere by cosmic radiation. *Physical Review* **83,** 1175–1188.

Stone, J. O., Allan, G. L., Fifield, L. K., and Cresswell, R. G. (1996). Cosmogenic chlorine-36 from calcium spallation. *Geochemica et Cosmochimica Acta* **60,** 679–692.

Stone, J. O., Evans, J. M., Fifield, L. K., Allan, G. L., and Cresswell, R. G. (1998). Cosmogenic chlorine-36 production in calcite by muons. *Geochemica et Cosmochimica Acta* **62,** 433–454.

Stuiver, M., and Reimer, P. J. (1993). Extended ^{14}C data base and revised CALIB 3.0 ^{14}C calibration program. *Radiocarbon* **35,** 215–230.

Stuiver, M., Reimer, P. J., Bard, E., Beck, J. W., Burr, G. S., Hughen, K. A., Kromer, B., McCormac, F. G., v. d. Plicht, J., and Spurk, M. (1998). INTCAL98 Radiocarbon age calibration 24,000—0 cal BP. *Radiocarbon* **40,** 1041–1083.

Swanson, T. W. (1994). "Determination of ^{36}Cl Production Rates from the Deglaciation History of Whidbey and Fidalgo Islands, Washington." Unpublished Ph.D. dissertation, University of Washington.

Swanson, T. W., Sharma, P., Phillips, F. M., and Zreda, M. (1992). Determination of Chlorine-36 production rates from the deglaciation history of Whidbey Island, WA. *Symposium on Accelerator Mass Spectrometry: Applications of Rare Isotopes as Tracers in Science and Technology, Division of Nuclear Chemistry and Technology*, San Francisco, California (abstract).

Thorson, R. M. (1980). Ice-sheet glaciation of the Puget Lowland, Washington, during the Vashon Stade (late Pleistocene). *Quaternary Research* **13,** 303–321.

Thorson, R. M. (1989). Glacio-isostatic response of the Puget Sound area, Washington. *Geological Society of America Bulletin* **101,** 1163–1174.

Thorson, R. M. (1993). Post glacial offset along the Seattle Fault. *Science* **260,** 825–826.

Tric, E., Valet, J. P., Tucholka, P., Paterne, M., Labeyrie, L., Guichard, F., Tauxe, L., and Fontugne, M. (1992). Paleo-intensity of the geomagnetic field during the last eighty thousand yr. *Journal of Geophysical Research* **97,** 9337–9351.

Yamashita, M., Stephans, L. D., and Patterson, H. W. (1966). Cosmic-ray produced neutrons at ground level: Neutron flux rate and flux distribution. *Journal of Geophysical Research* **71,** 3817–3834.

Zreda, M. G. (1994). "Development and Calibration of Cosmogenic ^{36}Cl Method and Application to Chronology of Late Quaternary Glaciations." Unpublished Ph.D. dissertation, New Mexico Institute of Mining and Technology.

Zreda, M. G., Phillips, F. M., Elmore, D., Kubik, P. W., and Sharma, P. (1991). Cosmogenic chlorine-36 production rates in terrestrial rocks. *Earth and Planetary Science Letters* **105,** 94–109.